Journal of CO2 Utilization 99 (2025) 103157

Contents lists available at ScienceDirect

Journal of CO2 Utilization

journal homepage: www.elsevier.com/locate/jcou

Techno-economic assessment of an integrated GTL facility for urea production

Kelvin Awani [a,*], Navid Khallaghi [a], Vinod Kumar [a,b], Seyed Ali Nabavi [a]

[a] Energy and Sustainability Theme, Cranfield University, Cranfield, Bedfordshire MK43 0AL, UK
[b] Magan Centre for Applied Mycology, Cranfield University, Cranfield MK43 0AL, United Kingdom

ARTICLE INFO

Keywords:
Decarbonisation
Gas-to-Liquid (GTL)
Hydrogen utilisation
Circular carbon economy
Techno-economic optimization

ABSTRACT

Decarbonising industrial processes remains a critical challenge, particularly in gas-to-liquid (GTL) and chemical manufacturing sectors. This study conducts a comprehensive techno-economic assessment of an integrated GTL-urea facility that leverages hydrogen from Fischer-Tropsch (FT) tail gas and green hydrogen via proton exchange membrane (PEM) electrolysis. Using ASPEN Plus simulations, process synergies, emission reductions, and profitability are analysed across multiple configurations. Key findings indicate that utilising internally generated hydrogen is more cost-effective, achieving a 4 % reduction in equipment costs, lowering total equipment cost from $2.58 billion in the base case to $2.47 billion. This results in a total annualised cost saving of $225 million and a 32 % increase in profitability, raising annual profits from $412 million in the base case to $543 million.

The integration efficiently repurposes CO_2 emissions and nitrogen-rich waste streams to produce urea, demonstrating strong potential for promoting circularity . It enhances carbon efficiency to 84 % reducing overall emission from 180 tonnes CO_2e/h in the business-as-usual case to 135 tonnes CO_2e/h while PEM-based hydrogen reduces emissions by 14 tonnes CO_2e/h compared to internally generated hydrogen. The high capital and operational costs due to electricity demands for PEM-based hydrogen process limit its viability. The study identifies the 9 tonnes/h internally generated hydrogen configuration as the optimal solution, offering significant emission reductions and financial benefits. These findings highlight the importance of process integration, renewable energy, and advanced hydrogen strategies for industrial decarbonisation, providing a sustainable pathway for GTL and urea production in line with global net-zero goals.

1. Introduction

Global industrial sectors, particularly energy, transportation, and manufacturing, contribute significantly to anthropogenic greenhouse gas (GHG) emissions, with accounting for nearly 79 % of the total global CO2 emissions [1]. Carbon capture and utilisation (CCU) strategies have emerged as promising alternatives to mitigate emissions, converting CO_2 into valuable products like methanol, urea, and synthetic fuels. Despite ongoing innovations, critical gaps remain in integrating these strategies into industrial processes while maintaining economic feasibility [2].

Green hydrogen production through renewable-powered electrolysis has emerged as a critical technological intervention, demonstrating significant potential for industrial decarbonisation. Advanced electrolysis technologies have systematically addressed historical challenges, including reducing capital investment costs, enhancing energy conversion efficiency, and improving reliability. Hydrogen purification technologies have simultaneously advanced, developing novel membrane and adsorption methodologies capable of achieving exceptional purity levels exceeding 99.99 % [3–6]. These innovations represent transformative breakthroughs in industrial gas processing, enabling more sophisticated hydrogen utilisation strategies across multiple industrial sectors, including GTL [3–6].

Previous studies have explored various approaches to improve GTL processes and ammonia-urea synthesis. For instance, the research by Rafiee et al. [7] examines integrating an FT GTL plant with a co-located power station using captured CO_2 from the power plant in steam or auto-thermal reformers. The simulation prioritised wax production, showing that while the ATR (auto thermal reformer) process has minimal CO_2 intake flexibility, the Steam Methane Reforming (SMR) process can fully utilise the additional 105.5 tonnes/h CO_2. Similarly, Ziaei and colleagues [8] demonstrated the potential of ammonia-urea integration to reuse CO_2 and improve process economics. Using solar-powered

* Corresponding author.
E-mail address: kelvin.awani@cranfield.ac.uk (K. Awani).

https://doi.org/10.1016/j.jcou.2025.103157
Received 25 March 2025; Received in revised form 9 June 2025; Accepted 12 June 2025
Available online 21 June 2025
2212-9820/© 2025 The Author(s). Published by Elsevier Ltd. This is an open access article under the CC BY license (http://creativecommons.org/licenses/by/4.0/).

hydrogen production, optimisation showed that the iron-based setup produces 48 t/h of urea with consumption of 35 t/h of CO_2. In contrast, the cobalt-based setup offers higher profitability, carbon efficiency, and urea output but lower wax production. Panahi et al. [2] integrated the GTL process with ammonia and urea synthesis units to utilise CO_2 emissions from the GTL process for urea production. Optimisation maximises carbon efficiency and wax production, using variables such as gas recycling ratios and CO_2 intake. The integration produces 434,000 tonnes of urea annually, utilising 37 tonnes of GTL CO_2 emissions per hour, and enhances profitability by 8 %. Rafiee et al. [9,12] examine CO_2 hydrogenation to methanol, optimising reactor productivity, CO_2 utilisation, and hydrogen conversion. Results show that an inlet H_2/CO_2 ratio of 3 improves methanol production by 59 % and boosts hydrogen and CO_2 conversion compared to a ratio of 2. However, a higher H_2/CO_2 ratio increases natural gas consumption and CO_2 emissions in conventional processes. If hydrogen is sourced via water electrolysis, the CO_2 hydrogenation process achieves negative emissions.

Autothermal reforming with carbon capture and storage (CCS) enables efficient, low-carbon hydrogen production from hydrocarbons by capturing associated CO_2 emissions, it can be integrated with alkaline electrolysis to provide complementary renewable-powered hydrogen generation during peak electricity periods. This integrated approach combines the reliability of conventional reforming with the flexibility of electrolytic systems, offering a scalable pathway toward sustainable hydrogen economy implementation.

Previous studies have explored using green hydrogen from electrolysis and external CO_2 from co-located facilities to generate urea. While green hydrogen production via electrolysis is heralded as a sustainable solution, its high energy demands, and infrastructure costs present considerable economic challenges [10]. Additionally, integrating externally sourced CO_2 into a GTL facility can be prohibitively expensive if the facilities are not nearby. This study addresses these gaps by presenting an integrated GTL-urea facility that utilises waste streams from GTL, like hydrogen from FT tail gas (Internally generated hydrogen), waste nitrogen from Air separation unit (ASU) and CO_2 in tail gas to produce ammonia and urea. By comparing internally generated hydrogen with PEM-based green hydrogen, the research evaluates the techno-economic implications of both configurations. The solution integrates circular carbon principles, using waste nitrogen and CO_2 streams from GTL processes to optimise resource utilisation. The analysis focuses on reducing emissions, maximising profitability, and overcoming cost barriers associated with green hydrogen, thereby advancing a pathway for sustainable industrial operations, this work did not examine other sustainable pathway for hydrogen production like biomass-to-hydrogen [40,41].

1.1. Process description

Process boundary conditions from the 34,000 bbl/day Oryx GTL plant in Qatar were used as the basis for the ASPEN PLUS process simulation of the GTL ASU, FT reactor, ATR, and utility steam furnace. A rich FT overhead tail gas composition was assumed. The simplified process flow schematic for the integrated GTL and Ammonia/Urea production system is shown in Fig. 1.

Ambient air is compressed, liquefied, and cryogenically distilled to produce high-purity gaseous oxygen required to oxidise natural gas in the ATR reactor partially. The cryogenic distillation cold box separates air at temperatures around −160°C, exploiting the difference in liquefaction temperatures of O_2 and N_2 [11]. A slipstream of the N_2 produced by the ASU is utilised as seal gas, process purge for inerting, and startup heating medium. Over 94 % of the nitrogen is vented as waste. However, the integrated GTL facility repurposes this waste nitrogen for ammonia production.

The syngas generation unit employs the ATR process, which combines SMR and Partial Oxidation (POx) to convert natural gas into a mixture of hydrogen (H_2) and carbon monoxide (CO) in a 2:1 ratio, known as synthesis gas (syngas). The natural gas (NG) feed for the ATR unit is initially heated to approximately 355°C in the ATR furnace chamber. This facilitates the conversion of organic sulphur compounds in the NG feed into inorganic sulphur (H_2S) in the presence of hydrogen and a hydrogenation catalyst. The desulphurisation unit then adsorbs all the produced H_2S to prevent sulphur-induced deactivation of catalysts in

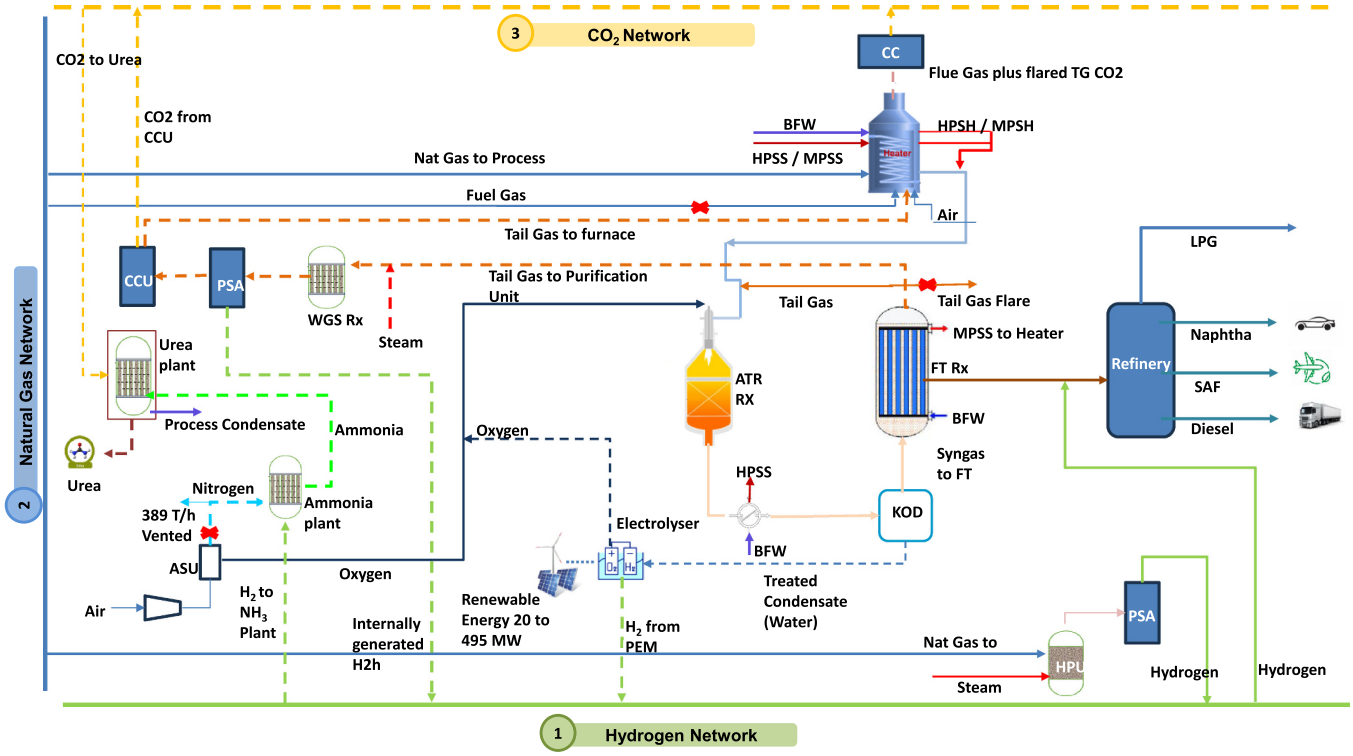

Fig. 1. Simplified process flow diagram for urea production via an integrated GTL.

downstream Fischer-Tropsch (FT) and hydro-processing units.

The desulphurised NG is subsequently pre-reformed to remove the C_{2+} fraction in the NG feed through SMR Eq. 1 and water-gas shift (WGS) Eq. 2 reactions in the presence of high-pressure superheated (HPSH) steam. The pre-reformer operates as an adiabatic reactor, modelled at a temperature of 455°C [15].

$$\text{for n} \geq 2: \quad C_nH_m + \text{n}H_20 \rightarrow (\text{n} + \quad 0.5\text{m})H_2 \quad + \text{nCO}\Delta H_{298K} = -1175\text{kJmol}^{-1} \tag{1}$$

$$CO + H_2O \leftrightarrow CO_2 + H_2 \quad \Delta H_{298K} = 41\text{kJmol}^{-1} \tag{2}$$

The ATR reactor automatically ignites the pre-reformed NG in pure O_2 and HPSH steam. The combustion of NG with oxygen as the limiting reactant, as shown in Eq.3, is referred to as POx. This exothermic reaction is accompanied by the endothermic reforming reaction Eq. 4 and the water-gas shift (WGS) reaction Eq. 2. To prevent the unwanted Boudouard soot formation reaction Eq. 5, a commercially proven overall steam-to-carbon ratio of 0.6 is maintained. This ratio includes steam supplied to the pre-reformer, ATR, and burner protection systems relative to the total carbon in the NG and recycled FT overhead stream.

$$CH_4 + 1.5O_2 \leftrightarrow CO + 2H_2O\Delta H_{298K} = 520\text{kJmol}^{-1} \tag{3}$$

$$CH_4 + H_2O \leftrightarrow CO + 3H_2 \quad \Delta H_{298K} = -206\text{kJmol}^{-1} \tag{4}$$

$$2CO \leftrightarrow CO_2 + C\Delta H_{298K} = 172.5\text{kJmol}^{-1} \tag{5}$$

Further pre-heating of the pre-reformer outlet using a furnace is necessary to achieve the desired ATR feed inlet temperature of 620–675°C. The ATR feed temperature directly influences the oxygen flow rate; lower feed temperatures require higher oxygen input to attain the target ATR outlet temperature of 1020–1050°C [13–15].

Pre-heating is achieved via a dual chamber furnace in Fig. 2

Approximately 1 % of methane is left unconverted to ensure complete oxygen conversion within the reactor. The H_2:CO ratio in the syngas is adjusted by increasing the flow of the FT overhead unconverted tail gas stream, which contains CO and CO_2. To enhance overall thermal efficiency, waste heat from the syngas exiting the ATR is utilised to heat boiler feed water (BFW) in a waste heat boiler and steam drum configuration. This process generates high-pressure saturated steam (HPSS), which is further heated to produce high-pressure superheated (HPSH) required to drive turbines and support the ATR process. The syngas is then cooled further to facilitate the removal of water produced during the ATR POX reaction Eq. 3 using a knockout drum (KOD). The presence of water in the syngas supplied to the FT process can damage the FT catalyst.

The cobalt-based FT reactor was modelled using a continuous stirred tank reactor (CSTR) and Iglesia's kinetic model, operating at 210°C and 21 bar, within the process's valid range. The exothermic reaction between the syngas feed and the FT catalyst produces hydrocarbons, with chain length determined by the oligomerisation reaction Eq. 6, yielding long-chain paraffin and olefins—the methanation reaction Eq. 7 also generates methane as a by-product.

$$\text{nCO} + 2\text{n}H_2 \quad \rightarrow \quad (- \quad CH_2)n + nH_2O \tag{6}$$

$$CO + 3H_2 \leftrightarrow CH_4 + H_2O \tag{7}$$

$$W_n \quad = n(1-\alpha).^2\alpha^{n-1} \tag{8}$$

$$\alpha = \frac{K_1P_{CO}}{K_1P_{CO} + \quad K_2P_{H2} + \quad K_3} \tag{9}$$

The WGS reaction is a crucial step in FT synthesis, serving as a reliable indicator of CO conversion, as one mole of CO reacts to produce one mole of water. The distribution of products between paraffin and olefins, along with the chain length, follows the Anderson-Schultz-Flory (ASF) model, as shown in (Eq.8), where n represents the number of carbon atoms, and *Wn* is the weight fraction. The probability of chain termination is (1-α), while α is the chain growth probability. As the H_2:CO (hydrogen to carbon monoxide) ratio in the syngas increases, α decreases, leading to the formation of shorter hydrocarbon chains in the LPG (C3-C4), Gasoline/Naphtha (C5-C11), Jet (C8 to C16) and Diesel (C12-C20) ranges. This reduces the weight fraction of heavier products in the wax range (C21 +). To enhance the profitability of the GTL process, longer-chain hydrocarbons in the wax range are preferred, as they can be cracked or hydrotreated to produce higher-value diesel products. The process of chain growth propagation is illustrated in Fig. 3.

The kinetic model in Eq. 9 determines the chain growth probability,

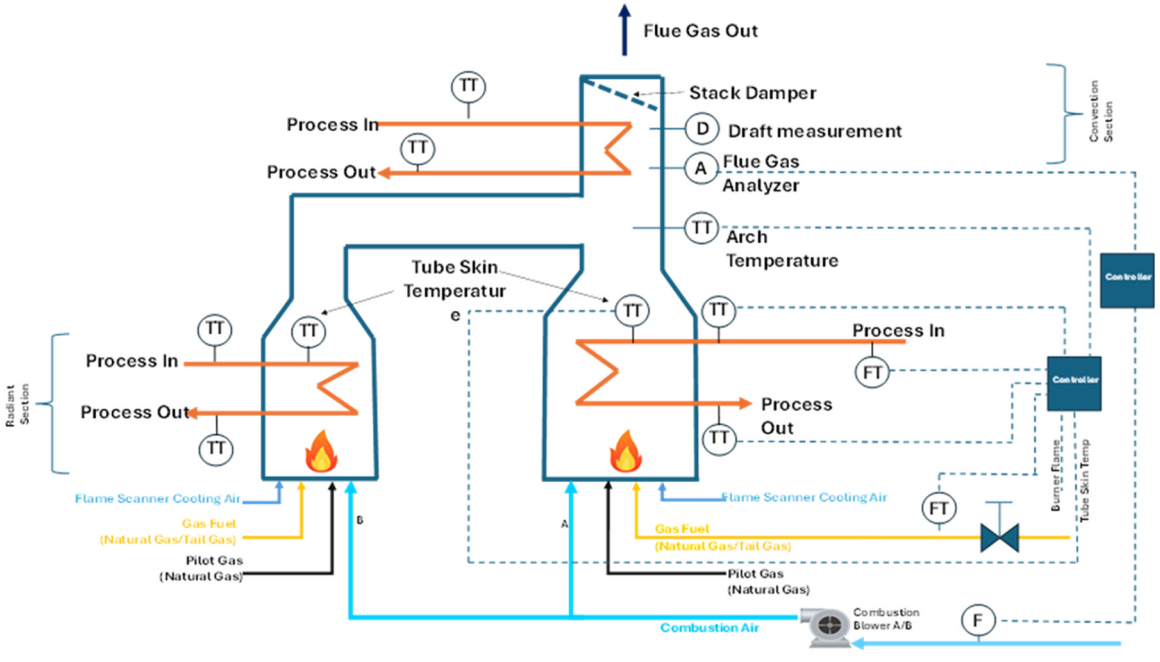

Fig. 2. The schematic of the dual chamber forced draft furnace.

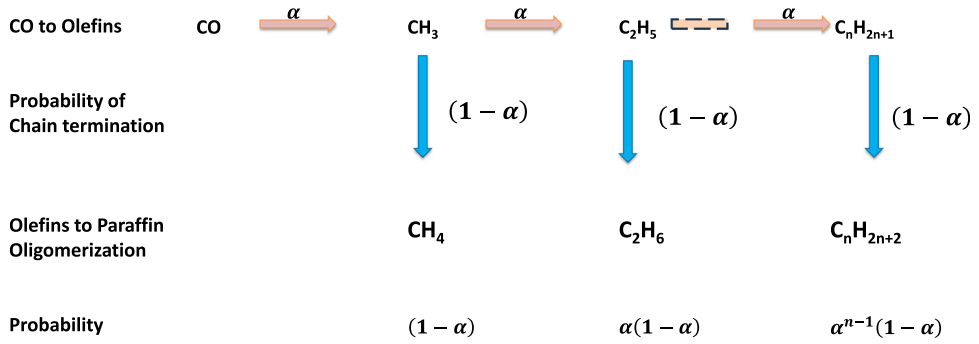

Fig. 3. Probability of chain growth progression from olefins to paraffins.

which uses the partial pressure of H_2 and CO and the K factors, which are functions of the operating temperature.

Nitrogen, hydrogen, and CO_2 are key feedstocks for urea production, a significant component of nitrogen-based fertilisers. In a GTL facility, all three feedstocks are internally generated. The integrated process generates these feeds: nitrogen is recovered from the ASU vent, and hydrogen is produced from the FT tail gas (TG) via the WGS reaction. This reaction shifts the CO conversion in the TG to CO_2, resulting in a 56 % increase in the hydrogen mole fraction, as shown in Eq. 2. The internally generated hydrogen is then separated from the TG stream using pressure swing adsorption, while the CO_2-rich tail gas is directed to a solid-based carbon capture adsorbent for further CO_2 capture.

Ammonia, produced via the Haber-Bosch process Eq. 10, is then combined with the captured CO_2 from the TG stream in the urea plant. The CO_2 reacts with ammonia to form carbamate Eq. 11, which is further converted into urea Eq. 12 [16]

$$3H_2 + N_2 \rightarrow 2NH_3 \quad \Delta H_{298K} = -91.8 \text{kJmol}^{-1} \tag{10}$$

$$2NH_3 + CO_2 \leftrightarrow H_2N - COOONH_4 \quad \Delta H_{298K} = -117 \text{kJmol}^{-1} \tag{11}$$

$$H_2N - COOONH_4 \leftrightarrow NH_2CONH_2 + H_2O \Delta H_{298K} = 16 \text{kJmol}^{-1} \tag{12}$$

The alternate hydrogen route is via water electrolysis using a PEM electrolyser module. The integrated GTL and urea plant would produce GTL (Diesel, SAF, light Naphtha in the (C5 to C9 range with the naphtha backend and diesel front end cut into jet fuel), LPG), ammonia, and urea.

1.2. Case configuration

Three distinct cases were evaluated: the business-as-usual base case, the integrated GTL with internally generated hydrogen case, and the integrated GTL with hydrogen from the PEM case for both GTL trains.

Business as usual (BAU) This case involves a standalone GTL and urea plant, as shown in Fig. 4. The GTL plant uses FT tail gas (TG) to reduce the H2:CO ratio in the ATR syngas, flaring the remaining TG. Additionally, 94 % of the nitrogen produced by the ASU is vented to the atmosphere.

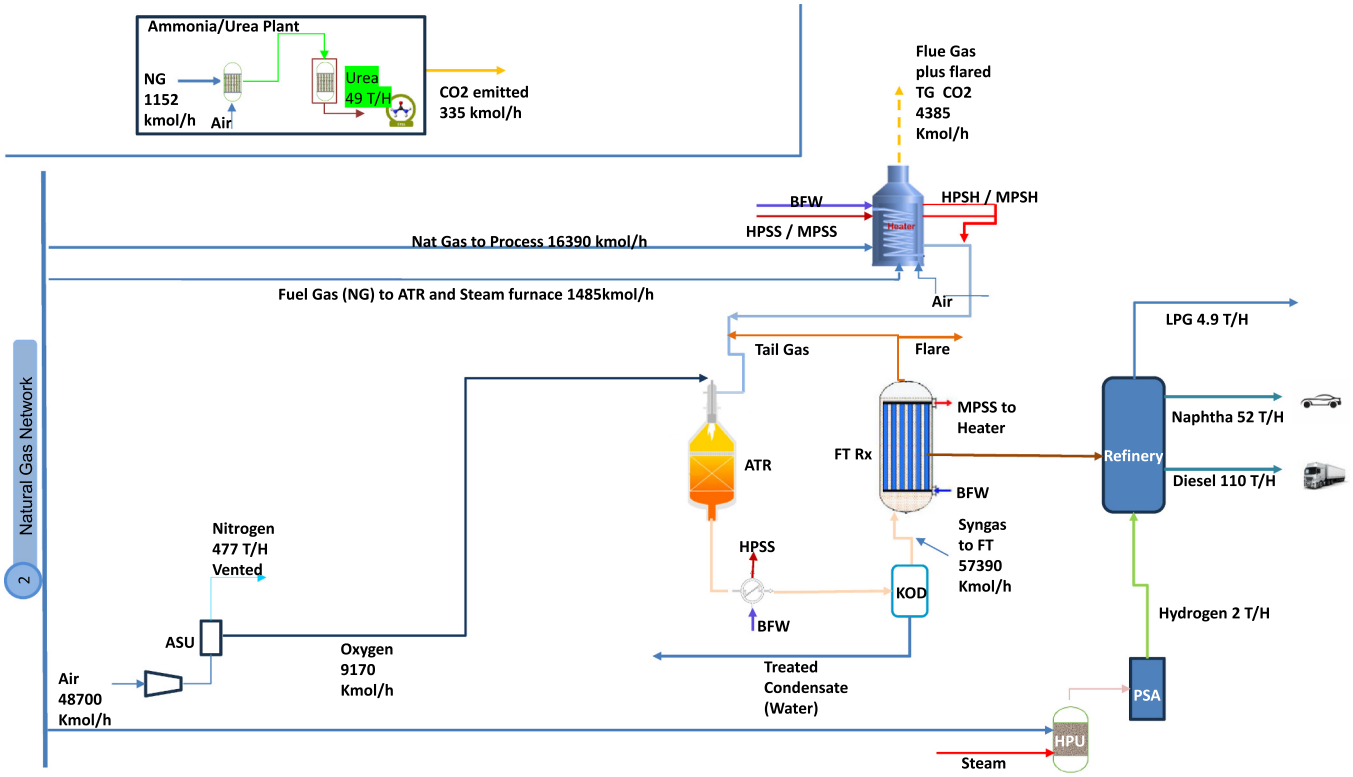

Fig. 4. BAU Standalone GTL and Urea Plant with no TG use in Furnace.

1.3. Base case

This case consists of a standalone GTL and Urea plant, as shown in Fig. 5. Flared TG in the BAU case is utilised in ATR and Steam generation furnaces. The GTL plant also utilises FT TG to reduce the ATR syngas H_2: CO ratio. 94 % of the nitrogen produced from ASU is vented to the atmosphere.

1.3.1. Integrated GTL with internally generated PSA hydrogen case (Case 3 to Case 8)

The GTL facility is integrated with the ammonia urea plant as shown in Fig. 6, with (6−9) t/h of hydrogen removed from the TG stream to furnace. The incremental steam required to fully convert the CO to CO_2 in the WGS reactor for additional hydrogen production is 40t/h, the WGS reaction would be needed if internally generated hydrogen requirement exceeds 6t/h. Case 3 to Case 8 evaluates the internal hydrogen case with varying TG flow to the ATR.

1.3.2. Integrated GTL with hydrogen from PEM case

This case integrates green hydrogen from PEM with the GTL facility as shown in Fig. 7.

1.4. Model development

For this study, the steady-state models for the ATR, FT, and steam generation furnaces were developed using Aspen Plus. The Peng-Robinson property method was applied to model the ATR and integrated processing unit, while the STEAMNBS steam table was used for the BFW/steam stream. Furnace heat, NG fuel, TG fuel, CO_2 composition in the furnace flue gas, and the pre-reformer composition were modelled using a Gibbs reactor to simulate thermodynamic equilibrium. The fuel sources (NG/TG) and combustion air were adjusted to maintain an excess O_2 target of 2.5–3 % in the flue gas and minimise the flue stack temperature, thereby improving overall thermal efficiency. The FT reactor was modelled as an isothermal CSTR, using the reaction rate proposed by Iglesia et al. [17,18] in combination with the ASF mass balance to simulate the reaction scheme and chain length propagation for C1, C2, LPG, Gasoline/Naphtha, and Wax. The assumptions for the rotating equipment are listed in Table 1.

The Aspen Plus model for the integrated ATR and furnace system was used to estimate the overall carbon intensity of the system. The process flow graphic output for the ATR system is shown in Fig. 8, with the furnace optimised as a Gibbs reactor using NG, TG, and air as feed. The unused radiant heat is recovered by convective coils, which preheat the desulphuriser inlet NG and hydrogen. The overall carbon intensity from the furnace flue gas, as depicted in Fig. 8, is validated based on the CO_2 equivalent of stream 8, with the percentage of excess oxygen in stream 8 maintained at 2.5 %.

The developed model compared green hydrogen from PEM and internally generated hydrogen from GTL FT TG integration for urea production as illustrated in the simplified process graphic in Figs. 9 and 10. Bottom of Form

1.5. Techno-economic performance indicators

The overall carbon intensity for each scenario is assessed using the Aspen Plus model, with the tonnes of CO_2e per hour emitted and utilised from the furnace flue stream and ATR consumption determined as model outputs. The steam requirement for the initial startup of the ATR and ASU was quantified using [2], while the fuel gas required for heating the steam generation and ATR feed pre-heating systems was calculated using Aspen Plus.

Carbon efficiency serves as a key performance indicator, evaluated as the proportion of carbon input (process natural gas feed and natural gas fuel for furnace) that is effectively utilised in the GTL/urea process to produce products, rather than being released as flared or vented emissions, it is defined in Eq. 18, the scope boundary for carbon accounting is limited to the GTL facility boundary scope 1 and 2 emissions, it did not consider upstream gas production, transportation and scope 3 activities.

The Total Annualized Cost (TAC) represents the overall cost of the

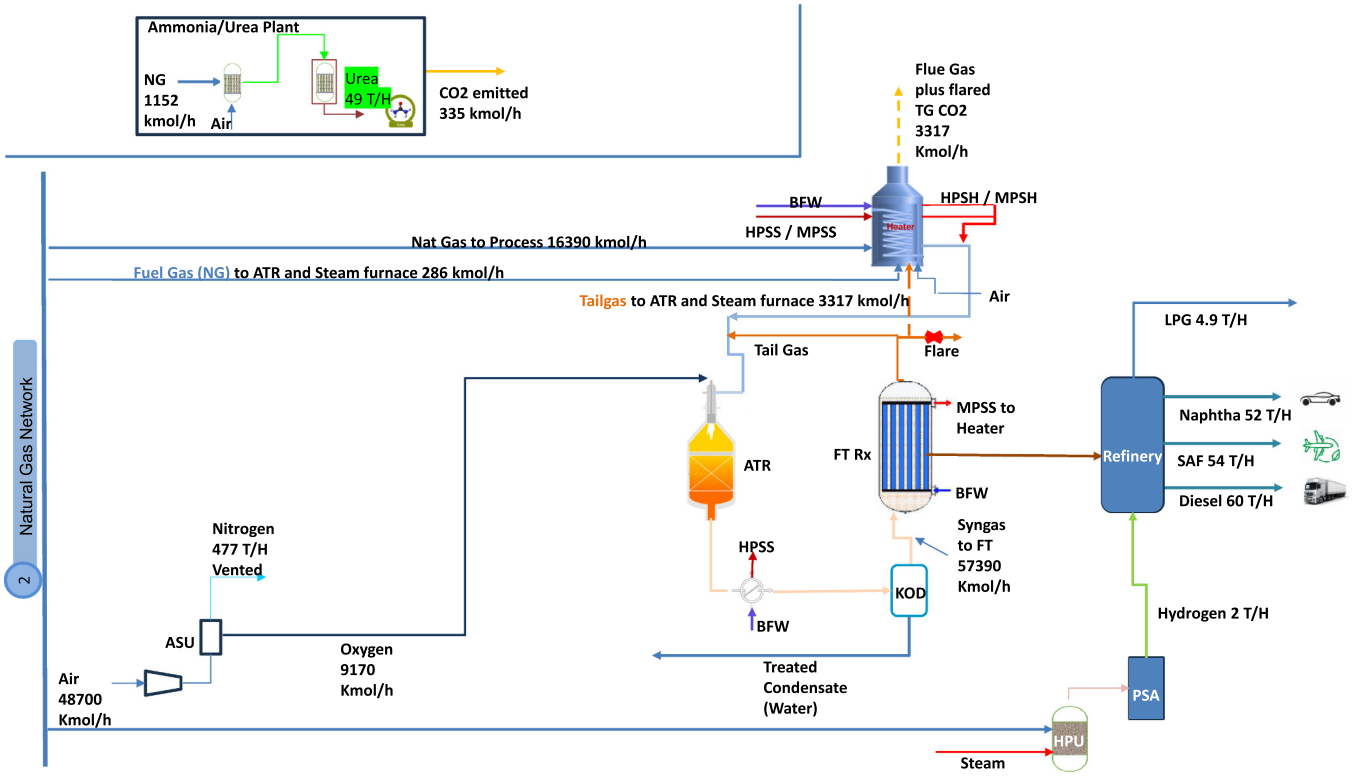

Fig. 5. Base Case standalone GTL and Urea plant with TG used in furnace.

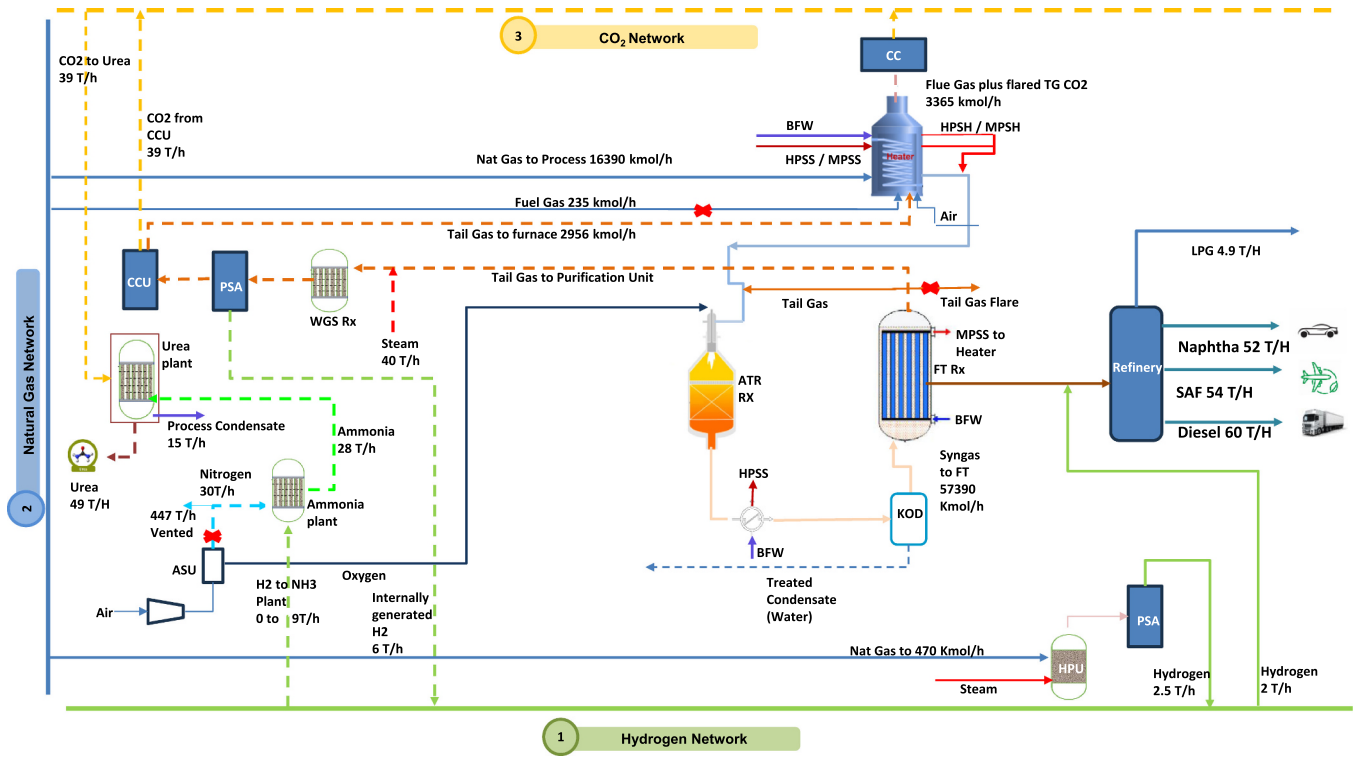

Fig. 6. Integrated GTL with internally generated hydrogen case.

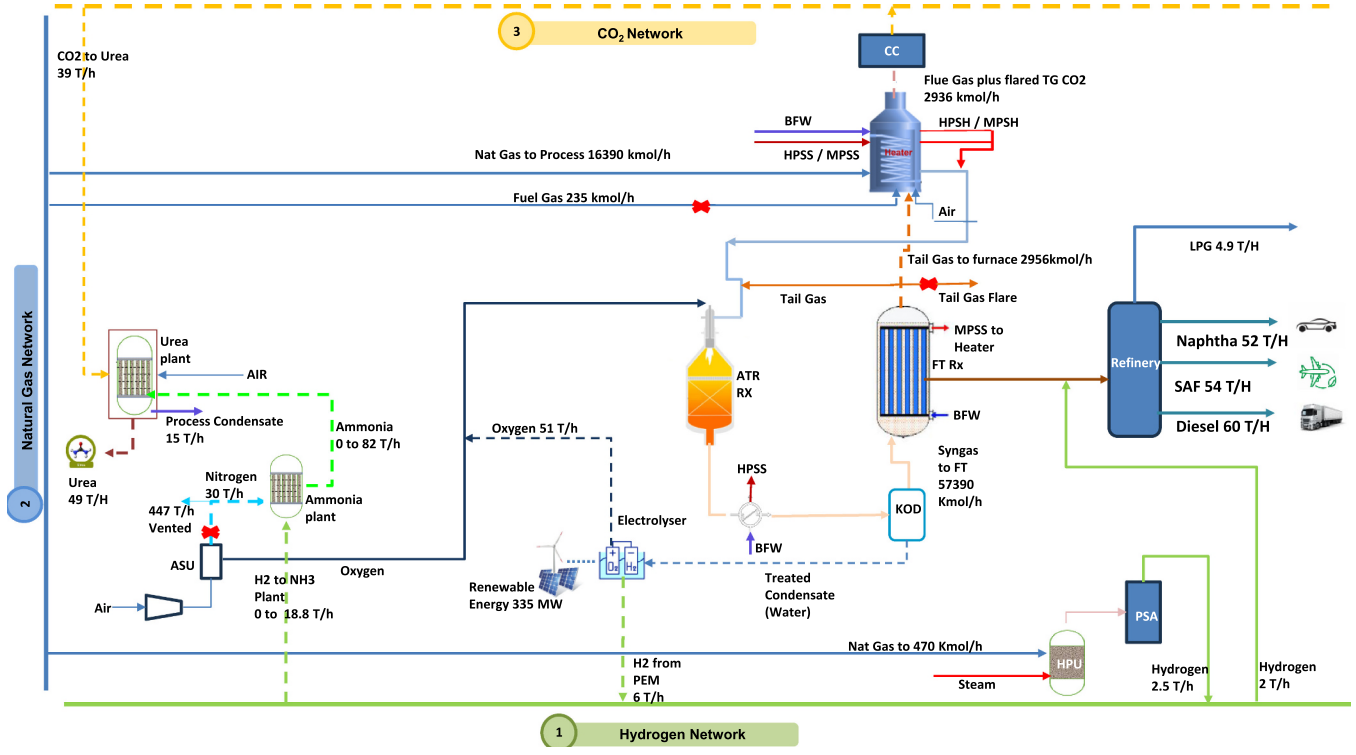

Fig. 7. Integrated GTL with hydrogen from PEM.

plant, including the Total Plant Cost (TPC), Fixed Capacity Factor (FCF), Variable O&M, and Fixed O&M costs. The Fixed Charge Factor (FCF), defined by Eq. 14, accounts for the project interest rate (r) and project lifespan (T). The Total Plant Cost (TPC) is the sum of the Indirect Capital Cost (ICC), Owner's Cost (OC), and Total Equipment Cost (TEC), with TEC being the total of all individual equipment capital costs (CB), as shown in Eq. 15

The equipment capital cost is calculated using reference equipment/plant costs and their respective capacities (CA and QA), along with a scaling factor (f) in Eq. 16. Annual revenue is determined by summing

Table 1
General assumptions for rotating equipment used in the simulation.

Parameters	Value	Reference
Compressors pressure ratio	1.8–2.7	[11]
Compressor Adiabatic Efficiency [%]	80	[11]
Isentropic efficiency of pumps [%]	90	[19]
Electrical efficiency of generators [%]	98.5	[20]
Pressure drop in heat exchanger [kpa]	10	[11]
Isentropic efficiency of expanders [%]	90	[19]
Isentropic efficiency of turbine [%]	89	[11]

the revenue from the sales of Diesel, Naphtha, LPG, and Urea, using the product prices listed in Table 2. A capacity factor of 80 % is applied to account for both planned and unplanned downtimes. Annual profit is calculated by subtracting the TAC from the annual revenue. The Profit Index (PI), given by Eq. 17, is determined for each Pareto front point, denoted as "i" in Eq. 17.

Techno-economic assessment formulas

$$TAC = TPC * FCF + Fuel\ Cost + Carbon\ tax + V_{OM} + \quad F_{OM} \tag{13}$$

$$FCF = \frac{r(1+r)T}{(1+r)T-1} \tag{14}$$

$$TEC = \sum_{i}^{n} C_{B,i} \tag{15}$$

$$C_B = \quad C_A \quad \left(\frac{Q_B}{Q_A}\right)^{\wedge f} \tag{16}$$

$$PI_i = \frac{(anual\ profit)_i}{Annual\ profit\ of\ the\ base\ case} \tag{17}$$

$$Carbon\ Efficiency = \frac{Carbon\ moles\ in\ final\ product}{Carbon\ mole\ in\ feed(process + fuel)} \tag{18}$$

The techno-economic assessment of each case was conducted based on the economic and CAPEX costing of new equipment, as outlined in Table 2, capital cost data for each sub-units are summarised in Table 3.

The impact of additional oxygen production from PEM was considered when evaluating the cost of ASU for both the integrated internally generated hydrogen and PEM hydrogen cases. The ASU plant size and cost are lower in the PEM case, as the oxygen produced by PEM was factored in. The utilised oxygen mass flow rate for the ATR is 81 kg/sec [25].

1.6. Model Verification

The integrated process model for the ATR reactor was validated with the pilot data from Haldor Topsoe combined partial oxidation and steam methane reforming data [14,21], where the pilot data for the commercialisation of ATR process was shared, the operating overall steam to carbon ratio of 0.6 is industrially proven to avoid carbon whiskers formation that propagates to soot, the H_2:CO ratio in the exit syngas is adjusted from 2.3 to 2 with FT tailgas from, the model aspen output achieved the same syngas H2:CO ratio for the steam, natural gas and oxygen feed. The maximum error in the model data shown in Fig. 11 and Appendix 2 compared to the pilot data is less than 2 %. The results of this study align with Case 2 from Rafie et al. [7], where tail gas from the FT overhead is utilised to adjust the syngas H_2:CO ratio, enhancing chain growth probability for increased wax production. The oxygen consumption in this research is 5236 kmol/h, closely matching that of HTAS while maintaining a syngas outlet temperature of 1050°C with less than 1 % methane slip. A CO_2-rich tail gas stream of 19,000 kmol/h, with all hydrogen removed, is introduced to adjust the syngas ratio. The composition of the tail gas after the water-gas shift (WGS) reactor, as shown in Fig. 1, is CO_2 60 %, CO 10 %, H_2 0.01 %, N_2 2 %, CH_4 23 %, and C_2+ 5 %. In comparison, the tail gas composition from the FT overhead consists of CO_2 33 %, CO 22.5 %, H_2 25 %, N_2 2 %, CH_4 15.5 %, and C_2+ 2 %.

Retrofitting internally generated hydrogen into an existing GTL facility involves a multi-stage process integration that requires significant

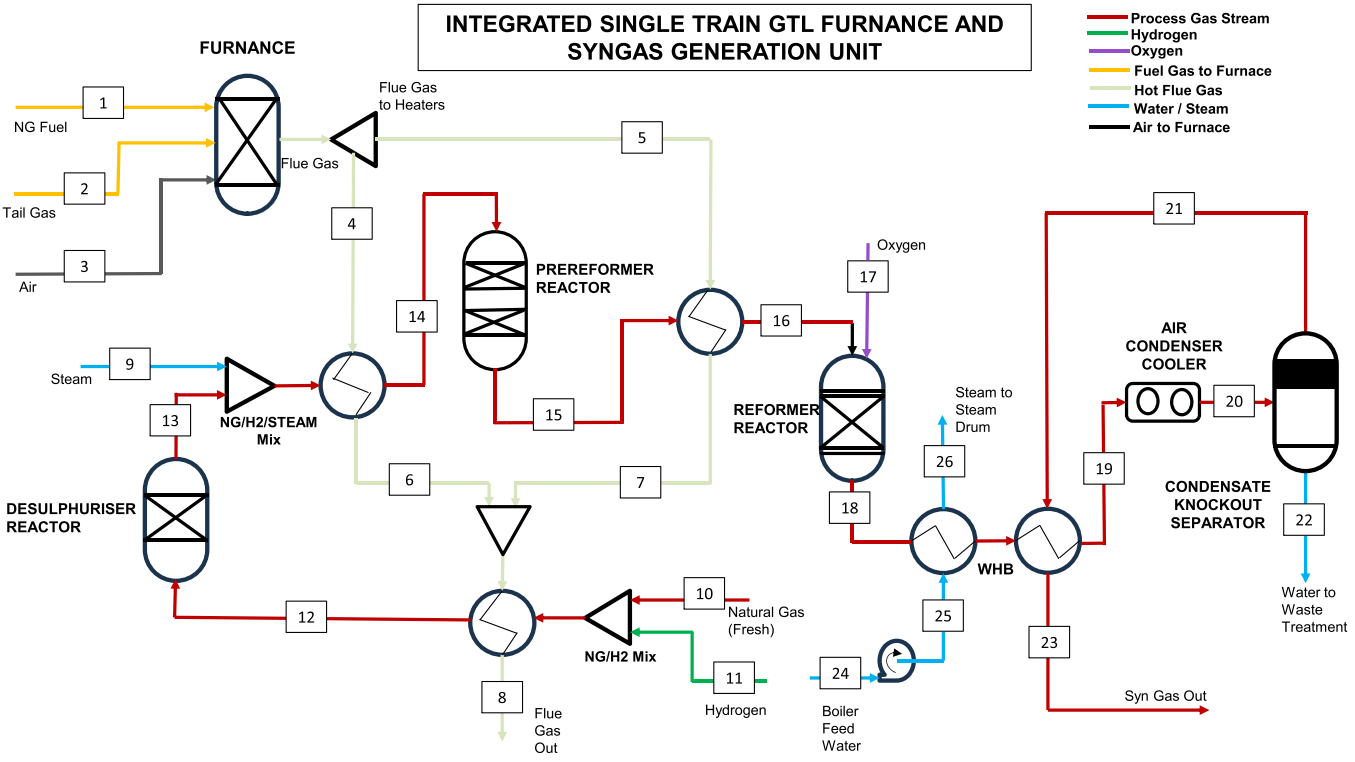

Fig. 8. Integrated GTL with hydrogen generated via PEM.

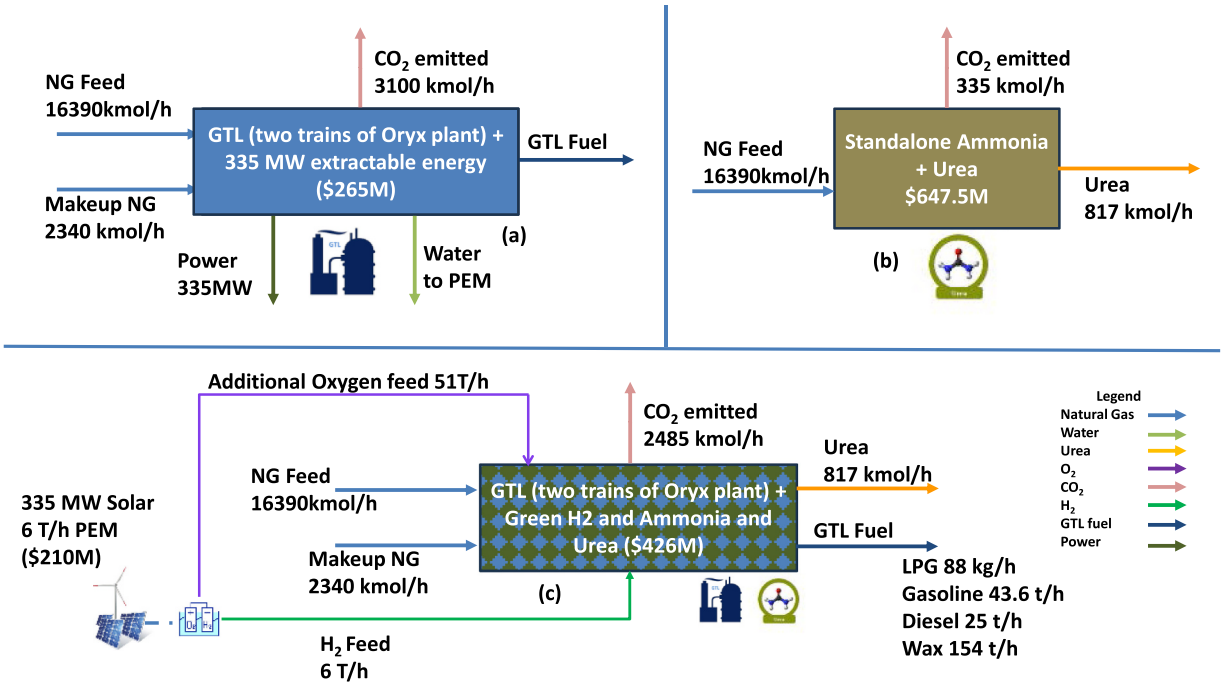

Fig. 9. Techno-economic evaluation for the integration of PEM generated green Hydrogen with GTL to produce urea [8].

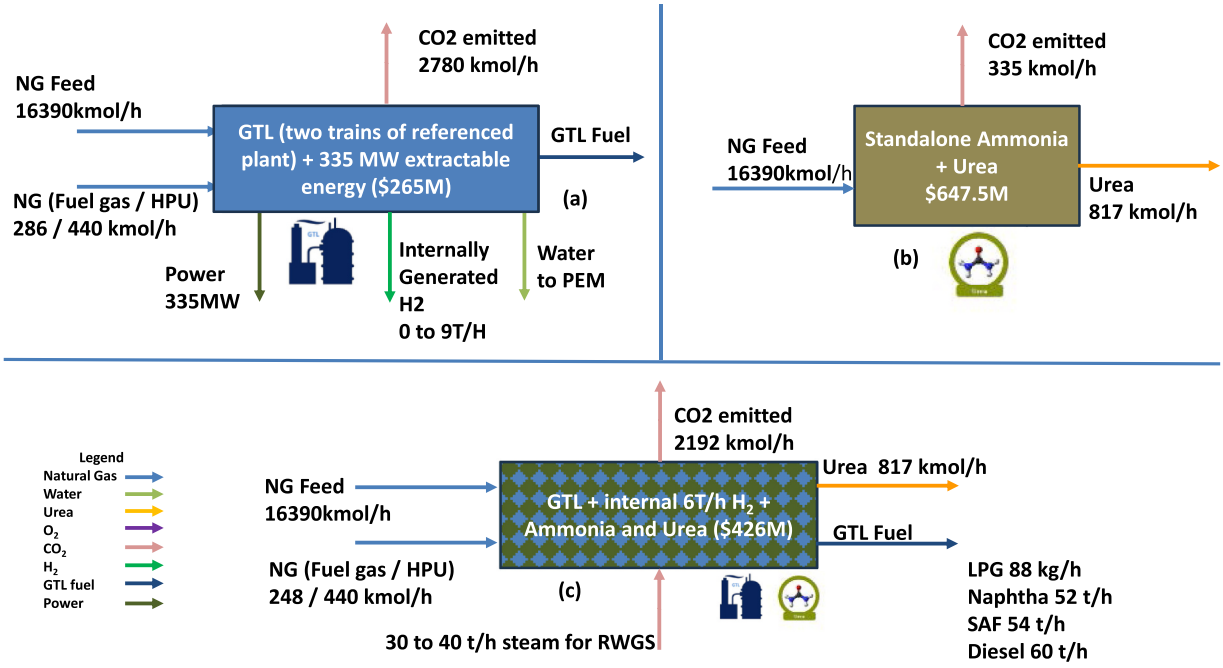

Fig. 10. Techno-economic evaluation for the integration of internally generated GTL Hydrogen with GTL to produce urea.

infrastructure modifications. The retrofit begins with diverting tail gas currently used as furnace fuel to a WGS reactor, which converts approximately 23 % CO content to CO_2 while producing additional H_2. This is followed by a solid sorbent-based CO_2 capture unit to separate CO_2 for urea synthesis, with the remaining stream processed through a hydrogen purification unit to produce pure hydrogen for ammonia production.

The retrofit demands substantial physical modifications including additional compressors to boost hydrogen and CO_2 feed pressures for urea synthesis, dedicated space allocation within the existing GTL facility for these new unit operations, and extensive additional infrastructure for ammonia and urea plants including storage tankage, piping networks, and utilities integration. The facility must accommodate this expanded footprint while maintaining existing GTL operations, requiring careful spatial planning, structural assessments, and potentially phased construction to minimise operational disruptions during the retrofit implementation.

The CAPEX economic assumption for the urea plant was validated with the recently completed 3 M mtpy Dangote fertiliser plant, and the variance between the assumption and reference plant was 7 %.

Table 2
Economic model assumptions.

Variables	Symbol	Unit	Value	Ref
Project Interest Rate	R	%	8	[22]
Project Lifetime	T	Yrs	30	[19]
Fuel/Natural Gas Cost	C_{fuel}	$/GJ	3	[19]
Indirect Capital Cost	ICC	% of TEC $	30	[23]
Owners Cost	OC	% of TEC	15	[19]
Fixed O&M cost	$F_{O\&M}$	% of TPC $	1	[24]
Variable O&M cost	$V_{O\&M}$	% of TPC $	2	[19]
Capacity Factor	CF	%	80	[19]
Fixed Charge Factor/Annual Capacity Charge	FCF		0.08	[19]
Labor cost		$/Person/year	85000	[19]
Plant Maintenance Cost		% of Capex/yr	3	[27]
EUR/USD Exchange rate			1	
Average Mol Weight of NG	Mwt NG	Kg/kmol	17	[28]
Average Price of Raw Materials and Products*				
Diesel/Jet		$/kg	0.8	
Naphtha		$/kg	0.6	
LPG		$/kg	0.5	
Electricity		$/KW	0.1	
CO_2 tax		$/tonne	0	
Natural Gas		$/GJ	4	
Urea		$/tonne	254	
Ammonia		$/tonne	262	
Oxygen		$/tonne	0.3	[29]
Calculated Cost of grey Hydrogen no CCS		$/KG	1.7	[30]
Calculated Cost of Hydrogen with CCS		$/KG	2.1	[30]
Calculated Cost of green Hydrogen with CCS		$/KG	3.6	[30]

* Product prices are from the I year average Nymex futures for European spec

2. Result and discussion

Two main objective functions were evaluated: one aimed at reducing the GTL/ integrated urea process's overall carbon emission footprint, and the other focused on maximising overall returns. Five independent variables were assessed within their lower and upper bounds, as shown in Table 4, The upper band limits were set by the maximum hydrogen that can be recovered from a two-train GTL FT TG system (4700 kmol/h), which determines the required CO2 removal from the tail gas and the overall urea production capacity. The resulting objective functions were calculated using a detailed Aspen Plus simulation, as presented in Table 5 with a detailed breakdown in Appendix A.

This study presents a techno-economic comparison of green hydrogen and internally generated hydrogen integration for urea production. A techno-economic evaluation by Ziaei et al. [8], depicted in Fig. 1, is compared with the findings of this research, illustrated in Figs. 9 and 10, which demonstrate the harmonised integration of internally generated hydrogen within the urea production process. The total annualised cost reported by Ziaei et al. is $225 million higher than that of this study, primarily due to the cost savings from avoiding green hydrogen production and its associated backup storage.

The profit index (Objective 1) is higher for the integrated GTL plant utilising internally generated hydrogen, as it avoids costs associated with PEM electrolysis, SMR for ammonia hydrogen production, ammonia gas sweetening, and refrigeration. The total equipment cost (TEC) for the 49 T/h urea integrated plant with internally generated hydrogen is 4 % lower, representing a savings of 110 million USD compared to the standalone base case. However, the TEC for the integrated plant using PEM is 15 % higher, resulting in an additional 390 million USD cost compared to the standalone base case. The higher cost for the integrated GTL with hydrogen produced via PEM is primarily due to the additional 335 MW of electricity required (1 MW of electricity generates 19 kg/h of H_2 and 151 kg/h of O2) [35], along with the cost of the PEM electrolysers. The 51 T/h of O2 produced from the PEM process would lead to a 17.5 % increase in GTL O2 production, which could help alleviate ASU constraints or reduce CAPEX for greenfield GTL plants. To generate the required 335 MW of electricity for PEM, 1674 acres of land would be needed (5 acres per MW) [38]. This land requirement could constrain PEM use in offshore or swamp-based GTL facilities, such as Escravos GTL, but may not be a concern for other onshore GTL projects [39].

Beyond space limitations, swamp-based GTL facilities face additional implementation challenges including elevated construction costs for solar mounting systems on unstable terrain, increased maintenance

Table 3
Scaling function for CAPEX calculation.

Sub System	Scaling basis	Reference Cost	Reference Capacity	Exponent Factor	Ref
Syngas Processing Unit	Mass Flow t/h – Syngas	6.6	20	0.55	[31]
Additional Power	Power Output MW	265	335	0.75	[26]
Capture Unit MDEA	Mass Flow t/h - CO_2	8.8	12.4	0.6	[23]
Carbon Processing Unit	Mass Flow t/h - CO_2	55.98	266.66	0.6	[31,32]
Hydrogen Purification Unit (PSA)	Mass Flow t/h – Hydrogen	18	20	0.7	[33]
Gas Turbine	Power MW	49.4	272.1	0.3	[33]
Heat Exchanger	Heat Transfer MW	6.1	828	0.67	[34]
Ammonia and Urea Plant	Urea Capacity [t/h]	647.5	49	0.68	[26]
Compressor	Power Kw	0.44	413	0.68	[31]
PEM Electrolyser	Installed Power MW	$1.5 * 10^6$	1	0.85	[35]
Shift Reactor	Mass Flow t/h - CO_2	48.53	54.4	0.75	[36]
ASU Plant Cost	Mass Flow t/day - O_2	19.1	325	0.7	[37]

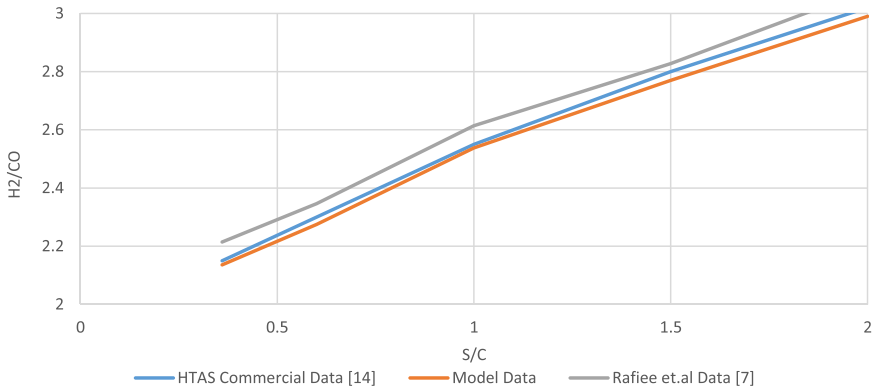

Fig. 11. H_2/CO ratio as a function of H_2O/C ratio in ATR outlet gas at 1050 °C.

Table 4
Integrated GTL multi-objective optimisation problem.

Objective functions				
Maximise Returns - Annual Profit Index		obj. 1		
Lower Carbon - Minimisation of CO_2 emissions		obj. 2		
Independent Variable	Lower Band	Upper Band	Units	Variable
CO_2 removed from FT TG	0	2607	kmol/h	A
Internal H_2 removed from FT TG by PSA	0	4700	kmol/h	B
Hydrogen from PEM	0	4700	kmol/h	C
Tail gas Utilisation (Furnace)	0	4000	kmol/h	D
Tail gas to ATR	0	6050	kmol/h	E

requirements due to high humidity and corrosive environments, potential wildlife habitat disruption, and complex permitting processes for environmental sensitive areas. These geographic constraints extend to other challenging locations such as offshore platforms (where space is extremely limited and harsh marine conditions prevail), urban industrial sites (with high land costs and zoning restrictions), and remote locations (lacking grid infrastructure for renewable energy integration). This analysis suggests that the viability of PEM-based green hydrogen integration is highly location-dependent, with onshore facilities in arid regions with abundant land and solar resources being more suitable, while space-constrained environments favour the internally generated hydrogen approach despite its higher carbon intensity, highlighting the need for site-specific techno-economic assessments that incorporate geographic and infrastructural realities into decarbonisation strategies. The carbon efficiency achieved in this research is 84 %, compared to 81 % in the previous study, mainly due to the near-complete utilisation (99 %) of produced tail gas, resulting in additional furnace fuel gas savings. The profit index in this study is 32 % higher than the base case, surpassing the findings of Ziaei et al. by 4 %. Furthermore, this study processes all 154 t/h of unconverted wax from Ziaei et al.'s work by recycling it to the front end of the hydro-processing unit. The jet slate in the diesel front end, determined by the boiling point (BP) curve for jet fuel (Initial BP 0 %, 147°C; Final BP 100 %, 254°C), is recovered from the diesel slate, which follows a boiling point curve of Initial BP 0 %, 165°C, and Final BP 100 %, 356°C. The backend of the naphtha C8 to C12 is pushed into the diesel and then to the Jet stream

The overall utilisation of tail gas (for the furnace and ATR) has a significant impact on the objective functions. Priority should be given to converting tail gas into product through its use in the ATR. Excess tail gas utilised in the furnace reduced natural gas (fuel gas) consumption from 1485 kmol/h to 286 kmol/h in the base case. Further optimisation in Cases (3–15) led to a decrease in natural gas flow to between 85 and 275 kmol/h. Consequently, natural gas OPEX costs fell from $4755/h to between $500 and $1200/h with the introduction of tail gas to the furnace, resulting in a corresponding reduction of 34–55 tonnes/h in CO_2 emissions. Fig. 12 (a–d) highlights the impact of tail gas utilisation in the furnace on natural gas consumption, OPEX, CO_2 emissions, and overall revenue.

For minimising carbon emissions (Objective 2), the carbon emissions in the integrated PEM case are slightly lower than in the integrated internal hydrogen case, primarily due to the additional 40 T/h steam requirement for the internal hydrogen WGS reaction. From an emissions perspective, utilising more TG in the ATR is significantly more efficient

Table 5
ASPEN Plus output of varying independent variables on the multi-objective.

Case Description	A	B	C	D	E	obj.1	obj. 2
BAU - Standalone GTL no TG Utilisation in furnace	0	0	0	0	5689	92	180
Base Case - Standalone GTL with TG Utilisation in furnace	0	0	0	3317	5689	100	136
3- Integrated GTL with 6 T/H internal H_2, with high TG to ATR	882	3181	0	2956	6050	125	138
4 - Integrated GTL with 6 T/H internal H_2, with low TG to ATR	882	3181	0	3817	5189	125	167
5 - Integrated GTL with 7.5 T/H internal H_2, with high TG to ATR	1054	3800	0	2956	6050	126	138
6 - Integrated GTL with 7.5 T/H internal H_2, with low TG to ATR	1054	3800	0	3817	5189	126	167
7 - Integrated GTL with 9 T/H internal H_2, with high TG to ATR	1304	4700	0	2956	6050	132	135
8 - Integrated GTL with 9 T/H internal H_2, with low TG to ATR	1304	4700	0	3817	5189	131	164
9 - Integrated GTL with 6 T/H_2 from PEM, with high TG to ATR	882	0	3181	2956	6050	103	121
10 - Integrated GTL with 6 T/H H_2 from PEM, with low TG to ATR	882	0	3181	3817	5189	103	155
11 - Integrated GTL with 7.5 T/H_2 from PEM, with high TG to ATR	1054	0	3800	2956	6050	101	121
12 - Integrated GTL with 7.5 T/H H_2 from PEM, with low TG to ATR	1054	0	3800	3817	5189	101	155
13- Integrated GTL with 9 T/H_2 from PEM, with high TG to ATR	1304	0	4700	2956	6050	99	118
14 - Integrated GTL with 9 T/H H_2 from PEM, with low TG to ATR	1304	0	4700	3817	5189	97	153
15 - Combined 9 T/H internal H_2 and 9 T/H h2 from PEM	2607	4700	4700	2956	6050	115	118

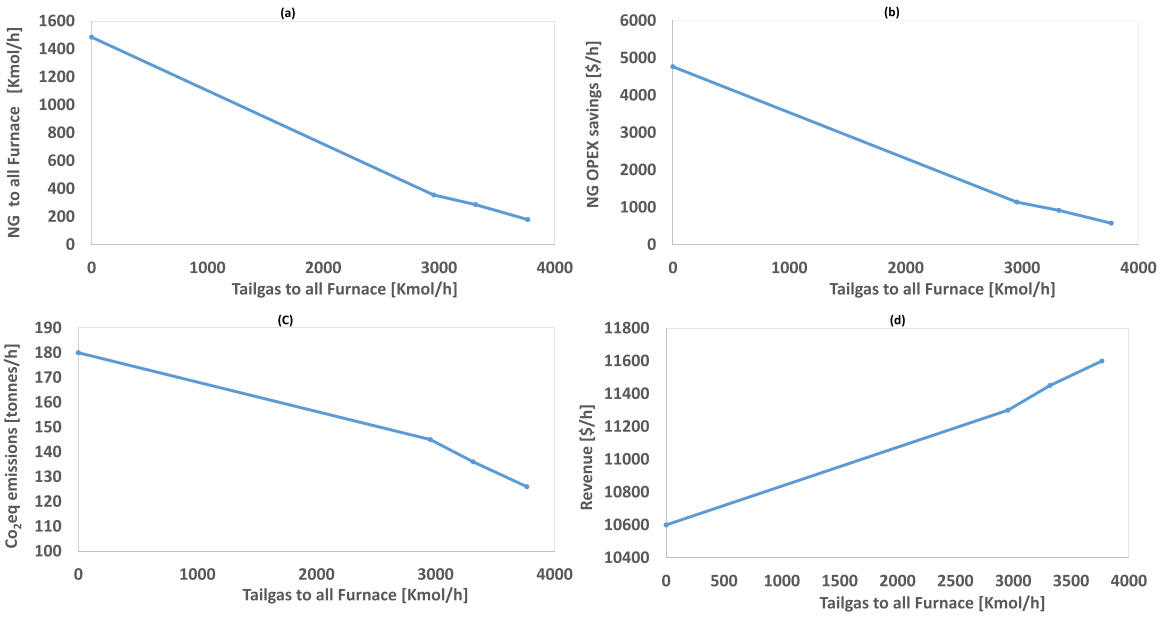

Fig. 12. Dependency of tailgas to GTL furnace with the objective functions.

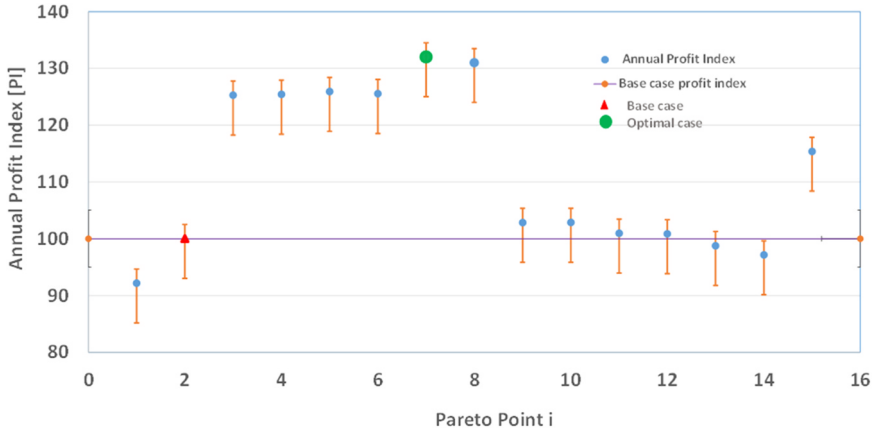

Fig. 13. Maximize Return - Integrating GTL facilities with Ammonia/Urea Plant.

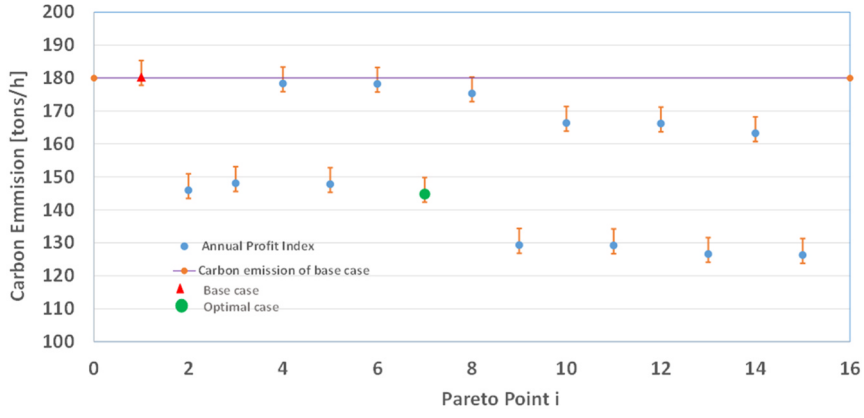

Fig. 14. Lower Carbon - Integrating GTL facilities with Ammonia/Urea Plant.

than flaring the TG. The evaluated alternatives are presented in Fig. 13 and Fig. 14 for both objective functions, the variation in annual profit is primarily driven by feed gas and hydrogen price, accounting for 3–10 % change in annual profit. Non-zero carbon tax and green hydrogen subsidies would significantly shift the economic balance in favour of the PEM-based hydrogen configuration. Currently, the study shows that internally generated hydrogen is more cost-effective due to PEM's high capital and operational costs, but carbon taxation would penalise the

Case	BAU	Base Case	3	4	5	6	7	8	9	10	11	12	13	14	15
CO_2 removed from FT TG Kmol/h	0	0	882	882	1054	1054	1304	1304	882	882	1054	1054	1304	1304	2607
H_2 Removed from FT TG Kmol/h	0	0	3181	3181	3800	3800	4700	4700	0	0	0	0	0	0	4700
H_2 from PEM	0	0	0	0	0	0	0	0	3181	3181	3800	3800	4700	4700	4700
TG Furnace	0	3317	2956	3817	2956	3817	2956	3817	2956	3817	2956	3817	2956	3817	2956
TG ATR	5689	5689	6050	5189	6050	5189	6050	5189	6050	5189	6050	5189	6050	5189	6050
Syngas	28695	28695	29109	28289	29385	28513	29493	28600	29109	28289	29385	28513	29493	28600	28880
2 TRAIN Syngas	57390	57390	58218	56578	58770	57026	58986	57200	58218	56578	58770	57026	58986	57200	57760
Additional O2 from PEM	0	0	0	0	0	0	0	0	1580	1580	1887	1887	2335	2335	2335
% ASU 2 train Capacity reduction	0	0	0	0	0	0	0	0	1580	1580	1887	1887	2335	2335	2335
NG to ATR Furnace Kmol/h	800	242	240	210	210	204	200	170	197	171	170	163	159	125	80
NG to Steam Superheater Kmol/h	445	20	18	18	18	18	6	6	18	18	18	18	6	6	3
NG to Steam Boilers Kmol/h	240	24	20	20	20	20	3	3	20	20	20	20	3	3	2
TG to ATR Furnace Kmol/h	0	1600	1450	2100	1450	2100	1450	2100	1450	2100	1450	2100	1450	2100	1400
TG to Steam Superheater Kmol/h	0	1150	1008	1150	1008	1150	1008	1100	1008	1150	1008	1150	1008	1100	706
TG to Steam Boilers Kmol/h	0	567	498	567	498	567	498	567	498	567	498	567	498	567	400
ATR Furnace Stack CO_2 Kmol/h	860	1600	1564	2103	1558	2100	1554	2098	1403	1945	1400	1941	1405	1938	1496
Steam Superheater Furnace Stack CO_2 Kmol/h	480	1150	1203	1303	1203	1303	1150	1250	1048	1248	1048	1248	995	1195	899
Steam Boilers Furnace Stack CO_2 Kmol/h	257	567	598	648	598	648	587	637	488	588	488	588	477	577	475
Syngas TRAIN CO_2	1635	1635	1898	1808	1871	1787	1902	1811	1890	1801	1865	1779	1892	1801	1801
Syngas 2 TRAIN CO_2	3270	3270	3796	3616	3742	3574	3804	3622	3780	3602	3730	3558	3784	3602	3602
H_2:CO	2	2	2	2	2	2	2	2	2	2	2	2	2	2	2
NG to all Furnace [GJ/H]	1485	286	278	248	248	242	209	179	235	209	208	201	168	134	85
Furnace NG Reduction [GJ/H]	0	1199	1207	1237	1237	1243	1276	1306	1250	1276	1277	1284	1317	1351	1400
Total Furnace Stack and TG flared CO_2 Kmol/h	4385	3317	3365	4054	3359	4051	3291	3985	2939	3781	2936	3777	2877	3710	2870
Ammonia produced Kmol/h	0	0	1634	1634	1952	1952	2414	2414	1634	1634	1952	1952	2414	2414	4828
UREA produced Kmol/h	0	0	817	817	976	976	1207	1207	817	817	976	976	1207	1207	2414
WATER from UREA Kmol/h	0	0	817	817	976	976	1207	1207	817	817	976	976	1207	1207	2414
DIESEL kg/h	110054	110054	109944	109834	109505	109176	108794	108413	108305	108196	108088	107980	107872	107764	107549
NAPHTHA kg/h	52031	52031	51979	51927	51771	51616	51435	51255	51204	51153	51102	51051	50999	50948	50847
LPG kg/h	4905	4905	4900	4895	4881	4866	4849	4832	4827	4822	4817	4813	4808	4803	4793
Urea Produced [t/h]	0	0	49	49	59	59	72	72	49	49	59	59	72	72	145
Cost of Urea/Ammonia in M$	648	648	648	648	731	731	845	845	648	648	731	731	845	845	1354
CO_2 to Urea [t/h]	0	0	39	39	46	46	57	57	39	39	46	46	57	57	115
PSA-H_2 to Urea [t/h]	0	0	6	6	8	8	9	9	0	0	0	0	0	0	9
Cost of FT Reactor M$	163	163	163	163	163	163	163	163	163	163	163	163	163	163	163
Cost of ATR M$	473	473	473	473	473	473	473	473	473	473	473	473	473	473	473
Oxygen Required in ASU t/h	292	292	292	292	292	292	292	292	241	241	231	231	217	217	217
Cost of ASU M$	164	164	164	164	164	164	164	164	143	143	139	139	133	133	133
Utilities and Refinery M$	1100	1100	1100	1100	1100	1100	1100	1100	1100	1100	1100	1100	1100	1100	1100
Cost of Integrated H_2-PSA+CCU M$	0	0	26	28	33	35	37	39	0	0	0	0	0	0	28
Compressors	0	0	17	18	18	20	20	21	0	0	0	0	0	0	23
Heat exchangers	0	0	8	8	9	9	9	10	0	0	0	0	0	0	10
Shift Reactor	0	0	38	38	43	44	51	52	0	0	0	0	0	0	85
CPU	0	0	18	18	20	20	22	23	0	0	0	0	0	0	34
Total BOP for GTL Ammonia/Urea M$	0	0	106	110	123	128	138	144	32	33	37	38	42	180	0
Integrated GTL /Urea Cost M$	648	648	542	539	609	604	707	701	616	615	695	693	804	1174	648
Additional MW Required	20	20	20	20	25	25	30	30	335	335	400	400	495	495	20
Cost of additional Electricity M$	32	32	32	32	38	38	43	43	265	265	303	303	355	355	32
Cost of Electrolyser M$	0	0	0	0	0		0		210	210	244	244	293	293	0
Total Equipment Cost M$	2580	2580	2474	2471	2547	2542	2650	2644	2971	2970	3117	3116	3321	3691	2580
Indirect Capital Cost M$	774	774	742	741	764	763	795	793	891	891	935	935	996	1107	774
Owners Cost M$	387	387	371	371	382	381	398	397	446	445	468	467	498	554	387
Total Plant Cost M$	3741	3741	3588	3582	3693	3685	3843	3833	4308	4306	4520	4518	4815	5352	3741
Annualized Plant Cost M$/y	309	309	296	296	305	304	317	316	356	355	373	373	397	442	309

(*continued on next page*)

(*continued*)

Case	BAU	Base Case	3	4	5	6	7	8	9	10	11	12	13	14	15
Annual NG Fuel Consumed GJ/y	12117600	2333760	2268480	2023680	2023680	1974720	1705440	1460640	1917600	1705440	1697280	1640160	1370880	693600	12117600
Fuel Cost M$/y	40	8	7	7	7	7	6	5	6	6	6	5	5	2	40
Fixed O&M $M	37	37	36	36	37	37	38	38	43	43	45	45	48	54	37
Variable O&M $M	75	75	72	72	74	74	77	77	86	86	90	90	96	107	75
Carbon Tax M$	0	0	0	0	0	0	0	0	0	0	0	0	0	0	0
Total Annualised Cost M$	461	429	411	410	422	421	438	436	491	490	514	514	546	605	461
Revenue from Diesel M$	594	594	593	593	591	589	587	585	584	584	583	583	582	580	594
Revenue from Naphtha M$	230	230	229	229	229	228	227	226	226	226	226	225	225	224	230
Revenue from LPG M$	17	17	17	17	17	17	17	17	17	17	17	17	17	17	17
Revenue from Urea M$	0	0	87	87	104	104	129	129	87	87	104	104	129	258	0
Annual Revenue M$	841	841	927	927	941	939	960	957	915	914	930	929	953	1080	841
Annual Profit M$	380	412	516	517	519	517	544	540	424	424	416	415	407	475	380
Profit Index Reference to Base Case	92	100	125	125	126	126	132	131	103	103	101	101	99	115	92
CO_2 Emission ton/h	180	136	138	167	138	167	135	164	121	155	121	155	118	118	180

higher emissions from internal hydrogen generation (14 tonnes CO2e/h more than PEM), making the cleaner PEM option more attractive despite its cost disadvantage.

Using internally generated hydrogen proves to be a more economical approach, leading to a 4 % reduction in equipment costs, with total equipment expenditure decreasing from $2.58 billion in the base case to $2.47 billion. This results in an annualised cost saving of $225 million and a 32 % boost in profitability, increasing annual profits from $412 million to $543 million.

3. Conclusion

This study demonstrates the techno-economic feasibility of integrating GTL facilities with urea production using internally generated hydrogen and green hydrogen from PEM electrolysis. Among the evaluated scenarios, the integration of GTL with internally generated hydrogen at 9 T/h emerges as the most balanced solution, delivering superior economic returns and significant carbon emission reductions. This configuration achieves a 20 % reduction in CO_2 emissions and a 32 % increase in annual profits compared to the base case. Feed gas and green hydrogen cost sensitivity accounts for the 3–10 % variation in annual profit, as shown in the Pareto front result in Fig. 13 and Fig. 14.

While green hydrogen integration offers slightly lower emissions, its higher capital and operational costs, driven by electricity consumption and electrolyser infrastructure, make it less economically competitive. However, its potential for ASU optimisation and CO_2 reduction remains valuable for specific applications, especially where land and renewable electricity resources are readily available.

The integrated GTL-urea system highlights the importance of process synergies in enhancing resource efficiency and profitability while addressing decarbonisation objectives. By leveraging waste streams such as FT tail gas and nitrogen from ASU, this approach supports a circular carbon economy and offers a robust pathway toward sustainable industrial operations.

CRediT authorship contribution statement

Navid Khallaghi: Writing – review & editing, Validation, Supervision, Methodology. **Awani Kelvin Offioritse:** Writing – review & editing, Writing – original draft, Visualization, Validation, Methodology, Investigation, Formal analysis, Data curation, Conceptualization. **Seyed Ali Nabavi:** Writing – review & editing, Validation, Supervision, Formal analysis, Data curation. **Vinod Kumar:** Writing – review & editing, Supervision, Conceptualization.

Declaration of Competing Interest

The authors declare that they have no known competing financial interests or personal relationships that could have appeared to influence the work reported in this article.

APPENDIX A. : simulation results for the multi-obj. responses to independent variable

Appendix 2. Tabular representation of validation data

Steam/Carbon	H_2/CO Commercial data	H_2/CO Model data	H_2/CO Rafie et.al data
0.360	2.150	2.136	2.215
0.600	2.300	2.275	2.346
1.000	2.550	2.538	2.614
1.500	2.800	2.770	2.828
2.000	3.020	2.990	3.080

Data availability

No data was used for the research described in the article.

References

[1] B. Parkinson, R.M. TJ, Comprehensive global industrial emissions analysis: sectoral mapping and carbon intensity evaluation, Nat. Clim. Chang (2024).

[2] M. Ziaei, M. Panahi, M.A. Fanaei, A. Rafiee, K.R. Khalilpour, 2019, Maximizing the profitability of integrated Fischer-Tropsch GTL process with ammonia and urea synthesis using response surface methodology 2019. https://doi.org/10.1016/j.jcou.2019.08.019..

[3] L. Zheng, WH, KR, Advanced membrane-based CO_2 separation technologies: polymer-ceramic composite membrane development for industrial applications, Chem. Eng. J. (2024).

[4] R. Gupta, SK, WH, Energy efficiency interventions in industrial processes: machine learning and digital twin optimization, Energy Effic. (2023).

[5] Chen C., Zhu X., Wen X., Zhou Y., Zhou L., Li H., et al. Coupling N 2 and CO 2 in H 2 O to synthesise urea under ambient conditions n.d. https://doi.org/10.1038/s41557-020-0481-9.

[6] S. Patel, C.L. KM, Advanced hydrogen purification methodologies: membrane and adsorption technology development, Sep Purif. Technol. (2024).

[7] A. Rafiee, M. Panahi, K.R. Khalilpour, CO_2 utilisation through integration of post-combustion carbon capture process with Fischer-Tropsch gas-to-liquid (GTL) processes, J. CO_2 Util. 18 (2017) 98–106, https://doi.org/10.1016/J.JCOU.2017.01.016.

[8] M. Ziaei, M. Panahi, M.A. Fanaei, A. Rafiee, K. Khalilpour, A highly carbon-efficient and techno-economically optimized process for the renewable-assisted synthesis of gas to liquid fuels, ammonia, and urea products, Int. J. Energy Res. 45 (2021) 16362–16382, https://doi.org/10.1002/ER.6886.

[9] A. Rafiee, Modelling and optimization of methanol synthesis from hydrogen and CO_2, J. Environ. Chem. Eng. 8 (2020) 104314, https://doi.org/10.1016/J.JECE.2020.104314.

[10] M. Panahi, A. Rafiee, S. Skogestad, M. Hillestad, A natural gas to liquids process model for optimal operation, Ind. Eng. Chem. Res 51 (2012) 425–433, https://doi.org/10.1021/ie2014058.

[11] Ebrahimi A., Meratizaman M., Reyhani H.A., Pourali O., Amidpour M. Energetic, exergetic and economic assessment of oxygen production from two columns cryogenic air separation unit 2015. https://doi.org/10.1016/j.energy.2015.06.083.

[12] H. Fazeli, M. Panahi, A. Rafiee, Investigating the potential of carbon dioxide utilisation in a gas-to-liquids process with iron-based Fischer-Tropsch catalyst, J. Nat. Gas. Sci. Eng. 52 (2018) 549–558, https://doi.org/10.1016/j.jngse.2018.02.005.

[13] T.S. Christensen, Adiabatic prereforming of hydrocarbons — an important step in syngas production, Appl. Catal. A Gen. 138 (1996) 285–309, https://doi.org/10.1016/0926-860X(95)00302-9.

[14] K. Aasberg-Petersen, J.-H. Bak Hansen, T.S. Christensen, I. Dybkjaer, P. S. Christensen, C. Stub Nielsen, et al., Technologies for large-scale gas conversion, Appl. Catal. A Gen. 221 (2001) 379–387, https://doi.org/10.1016/S0926-860X(01)00811-0.

[15] Aasberg-Petersen K., Christensen T.S., Nielsen C.S., Dybkjaer I. Recent developments in autothermal reforming and pre-reforming for synthesis gas production in GTL applications n.d. https://doi.org/10.1016/S0378-3820(03)00073-0.

[16] P.S. Varbanov, Q. Wang, M. Zeng, P. Seferlis, T. Ma, J.J. Klemeš, et al., Ammonia/urea production process simulation/optimisation applied techno-economic and

stochastic analysis, Chem. Eng. Trans. 81 (2020) 2020, https://doi.org/10.3303/CET2081198.
[17] E. Iglesia, S.C. Reyes, S.L. Soled, Reaction-transport selectivity models and the design of fischer–tropsch catalysts, Comput. Aided Des. Catal. (2020) 199–258, https://doi.org/10.1201/9781003067115-7.
[18] M. Panahi, A. Rafiee, S. Skogestad, M. Hillestad, A natural gas to liquids process model for optimal operation, Ind. Eng. Chem. Res. 51 (2012) 425–433, https://doi.org/10.1021/ie2014058.
[19] S. Ghiami, N. Khallaghi, T.N. Borhani, Techno-economic and environmental assessment of staged oxy-co-firing of biomass-derived syngas and natural gas, Energy Convers. Manag. 243 (2021) 114410, https://doi.org/10.1016/j.enconman.2021.114410.
[20] D.P. Hanak, V. Manovic, Economic feasibility of calcium looping under uncertainty, Appl. Energy 208 (2017) 691–702, https://doi.org/10.1016/j.apenergy.2017.09.078.
[21] K. Aasberg-Petersen, T.S. Christensen, C. Stub Nielsen, I. Dybkjær, Recent developments in autothermal reforming and pre-reforming for synthesis gas production in GTL applications, Fuel Process. Technol. 83 (2003) 253–261, https://doi.org/10.1016/S0378-3820(03)00073-0.
[22] N. Khallaghi, D. Hanak, V. Manovic, Techno-economic evaluation of near-zero CO_2 emission gas-fired power generation technologies_ a review _ Elsevier Enhanced Reader, J. Nat. Gas. Sci. Eng. (2020).
[23] N. Khallaghi, D.P. Hanak, V. Manovic, Techno-economic evaluation of near-zero CO_2 emission gas-fired power generation technologies: a review, J. Nat. Gas. Sci. Eng. 74 (2020) 103095, https://doi.org/10.1016/J.JNGSE.2019.103095.
[24] S. Mohajerani, A. Kumar, A.O. Oni, 2018, A techno-economic assessment of gas-to-liquid and coal-to-liquid plants through the development of scale factors 2018. https://doi.org/10.1016/j.energy.2018.03.005..
[25] A. Rafiee, M. Hillestad, Techno-economic analysis of a gas-to-liquid process with different placements of a CO $_2$ removal unit, Chem. Eng. Technol. 35 (2012) 420–430, https://doi.org/10.1002/ceat.201100418.
[26] M. Ziaei, M. Panahi, M.A. Fanaei, A. Rafiee, K.R. Khalilpour, Maximizing the profitability of integrated Fischer-Tropsch GTL process with ammonia and urea synthesis using response surface methodology, J. CO_2 Util. 35 (2020) 14–27, https://doi.org/10.1016/j.jcou.2019.08.019.
[27] Hanak D.P., Jenkins B.G., Kruger T., Manovic V. High-efficiency negative-carbon emission power generation from integrated solid-oxide fuel cell and calciner 2017. https://doi.org/10.1016/j.apenergy.2017.08.090.
[28] A. Rafiee, M. Hillestad, Synthesis gas production configurations for gas-to-liquid applications, Chem. Eng. Technol. 35 (2012) 870–876, https://doi.org/10.1002/CEAT.201100674.
[29] D. Bellotti, A. Sorce, M. Rivarolo, L. Magistri, Techno-economic analysis for the integration of a power to fuel system with a CCS coal power plant, J. V. Util. 33 (2019) 262–272, https://doi.org/10.1016/j.jcou.2019.05.019.
[30] J. Webb, T. Longden, F. Boulaire, M. Gono, C. Wilson, The application of green finance to the production of blue and green hydrogen: acomparative study, Renew. Energy 219 (2023), https://doi.org/10.1016/j.renene.2023.119236.
[31] A.M. Cormos, I. Dumbrava, C.C. Cormos, Evaluation of techno-economic performance for decarbonized hydrogen and power generation based on glycerol thermo-chemical looping cycles, Appl. Therm. Eng. 179 (2020) 115728, https://doi.org/10.1016/J.APPLTHERMALENG.2020.115728.
[32] D. Agrawal, K. Awani, S.A. Nabavi, V. Balan, M. Jin, T.M. Aminabhavi, et al., Carbon emissions and decarbonisation: the role and relevance of fermentation industry in chemical sector, Chem. Eng. J. 475 (2023) 146308, https://doi.org/10.1016/j.cej.2023.146308.
[33] M. Gazzani, D.M. Turi, G. Manzolini, Techno-economic assessment of hydrogen selective membranes for CO_2 capture in integrated gasification combined cycle, Int. J. Greenh. Gas. Control 20 (2014) 293–309, https://doi.org/10.1016/j.ijggc.2013.11.006.
[34] G. Manzolini, A. Giuffrida, P.D. Cobden, H.A.J. van Dijk, F. Ruggeri, F. Consonni, Techno-economic assessment of SEWGS technology when applied to integrated steel-plant for CO_2 emission mitigation, Int. J. Greenh. Gas. Control 94 (2020) 102935, https://doi.org/10.1016/j.ijggc.2019.102935.
[35] D. Bellotti, M. Rivarolo, L. Magistri, A.F. Massardo, Feasibility study of methanol production plant from hydrogen and captured carbon dioxide, J. CO_2 Util. 21 (2017) 132–138, https://doi.org/10.1016/j.jcou.2017.07.001.
[36] A. Naquash, M.A. Qyyum, Y.D. Chaniago, A. Riaz, F. Yehia, H. Lim, et al., Separation and purification of syngas-derived hydrogen: a comparative evaluation of membrane-and cryogenic-assisted approaches, Chemosphere 313 (2023) 137420, https://doi.org/10.1016/j.chemosphere.2022.137420.
[37] Rafiee A., Hillestad M. Techno-Economic Analysis of a Gas-to-Liquid Process with Different Placements of a CO 2 Removal Unit 2012. https://doi.org/10.1002/ceat.201100418.
[38] Solar Farmland Requirements: What Landowners Should Know n.d. ⟨https://lumifyenergy.com/blog/solar-farm-land-requirements/⟩ (accessed November 20, 2024).
[39] K. Awani, D. Hanak, V. Kumar, S.A. Nabavi, Techno-economic assessment of decarbonisation pathways for a gas to liquid facility: a review, J. Util. 90 (2024) 102994, https://doi.org/10.1016/J.JCOU.2024.102994.
[40] A. Hudha, E. Mohamed, E. Ahmed, Development of sustainable biogenic marine waste-based composite for phosphate ions recovery and subsequent biogas production, J. Biomass Bioenergy (June 2025) 107819, https://doi.org/10.1016/j.biombioe.2025.107819.
[41] M.G. Elaffy, E. Khalid, et al., Biomass-to-sustainable biohydrogen: Insights into the production routes, and technical challenges, Chem. Eng. J. Adv. (2022) 100410, https://doi.org/10.1016/j.ceja.2022.100410.

https://dspace.org/

Techno-economic assessment of an integrated GTL facility for urea production

Awani, Kelvin; Khallaghi, Navid; Kumar, Vinod; Nabavi, Seyed Ali

2025-09
Elsevier
https://doi.org/10.1016/j.jcou.2025.103157
Awani K, Khallaghi N, Kumar V, Nabavi SA. (2025) Techno-economic assessment of an integrated GTL facility for urea production. Journal of CO2 Utilization, Volume 99, September 2025, Article number 103157

Downloaded from a DSpace repository. https://dspace.org/